Application of the sextic oscillator with a centrifugal barrier and the spheroidal equation for some $X(5)$ candidate nuclei

2013 J. Phys. G: Nucl. Part. Phys. 40 025108

(http://iopscience.iop.org/0954-3899/40/2/025108)

J. Phys. G: Nucl. Part. Phys. **40** (2013) 025108 (29pp) doi:10.1088/0954-3899/40/2/025108

Application of the sextic oscillator with a centrifugal barrier and the spheroidal equation for some $X(5)$ candidate nuclei

A A Raduta[1,2] **and P Buganu**[1]

[1] Department of Theoretical Physics, Institute of Physics and Nuclear Engineering, POB MG-6, RO-077125, Romania
[2] Academy of Romanian Scientists, 54 Splaiul Independentei, Bucharest 050094, Romania

E-mail: raduta@nipne.ro

Received 27 September 2012
Published 16 January 2013
Online at stacks.iop.org/JPhysG/40/025108

Abstract
The eigenvalue equation associated with the Bohr–Mottelson Hamiltonian is considered in the intrinsic reference frame and amended by replacing the harmonic oscillator potential in the β variable with a sextic oscillator potential with centrifugal barrier plus a periodic potential for the γ variable. After the separation of variables, the β equation is quasi-exactly solved, while the solutions for the γ equation are just the angular spheroidal functions. An anharmonic transition operator is used to determine the reduced $E2$ transition probabilities. The formalism is conventionally called the sextic and spheroidal approach (SSA) and applied for several X(5) candidate nuclei: ^{176,178,180,188,190}Os, ^{150}Nd, ^{170}W, ^{156}Dy and ^{166,168}Hf. The SSA predictions are in good agreement with the experimental data of the mentioned nuclei. The comparison of the SSA results with those yielded by other models, such as $X(5)$ (Iachello 2001 *Phys. Rev. Lett.* **87** 052502), infinite square well (Raduta *et al* 2009 *Nucl. Phys.* A **819** 46) and Davidson like potential (Raduta *et al*) for the β, otherwise keeping the spheroidal functions for the γ , and the coherent state model (Raduta *et al* 1981 *Phys. Lett.* B **99** 444, Raduta *et al* 1982 *Nucl. Phys.* A **381** 253, Raduta *et al* 1987 *Phys. Rev.* C **36** 2111, Raduta *et al* 1983 *Z. Phys.* A **313** 69, Raduta *et al* 1997 *Phys. Rev.* C **55** 1747, Raduta *et al* 2002 *Phys. Rev.* C **65** 064322, Raduta and Sabac 1983 *Ann. Phys., NY* **148** 1, Raduta 2004 *Recent Research Developments in Nuclear Physics* vol 1) respectively, suggests that SSA represents a good approach to describe nuclei achieving the critical point of the $U(5)\rightarrow SU(3)$ shape phase transition.

(Some figures may appear in colour only in the online journal)

1. Introduction

Since the liquid drop model was developed [1], the quadrupole shape coordinates were widely used by both phenomenological and microscopic formalisms to describe the basic properties

of nuclear systems. Based on these coordinates, one defines quadrupole boson operators in terms of which model Hamiltonians and transition operators are defined. Since the original spherical harmonic liquid drop model was able to describe only a small amount of data for spherical nuclei, several improvements have been made. Thus, the Bohr–Mottelson model was generalized by Faessler and Greiner [2] in order to describe the small oscillations around a deformed shape which results in obtaining a flexible model, called vibration–rotation model, suitable for the description of deformed nuclei. Later on [3], this picture was extended by including anharmonicities as low-order invariant polynomials in the quadrupole coordinates. With a suitable choice of the parameters involved in the model Hamiltonian, the equipotential energy surface may exhibit several types of minima [4] such as spherical, deformed prolate, deformed oblate, deformed triaxial, etc. To each equilibrium shape, specific properties for excitation energies and electromagnetic transition probabilities show up. Due to this reason, one customarily says that static values of intrinsic coordinates determine a phase for the nuclear system. The boson description with a complex anharmonic Hamiltonian makes use of a large number of structure parameters which are to be fitted. A smaller number of parameters are used by the coherent state model (CSM) [5] which uses a restricted collective space generated through angular momentum projection by three deformed orthogonal functions of coherent type. The model is able to describe in a realistic fashion transitional and well-deformed nuclei of various shapes including states of high and very high angular momenta. Various extensions to include other degrees of freedom such as isospin [6], single particle [7] or octupole [8, 9] degrees of freedom have been formulated [10].

It has been noted that a given nuclear shape may be associated with a certain symmetry. Hence, its properties may be described with the help of the irreducible representation of the respective symmetry group. Thus, the gamma unstable nuclei can be described by the $O(6)$ symmetry [13], the gamma-rigid triaxial rotor by the $D2$ symmetry [14], the symmetric rotor by the $SU(3)$ symmetry and the spherical vibrator by the $U(5)$ symmetry. Thus, even in the 1950s, the symmetry properties have been greatly appreciated. However, a big push forward was brought by the interacting boson approximation (IBA) [15, 16], which succeeded to describe the basic properties of a large number of nuclei in terms of the symmetries associated with a system of quadrupole (d) and monopole (s) bosons which generate the $U(6)$ algebra of the IBA. The three limiting symmetries $U(5)$, $O(6)$ and $SU(3)$ mentioned above in the context of the collective model are also dynamic symmetries for $U(6)$. Moreover, for each of these symmetries a specific group reduction chain provides the quantum numbers characterizing the states, which are suitable for a certain region of nuclei. Besides the virtue of unifying the group theoretical descriptions of nuclei exhibiting different symmetries, the procedure defines very simple reference pictures for the limiting cases. For nuclei lying close to the region characterized by a certain symmetry, the perturbative corrections are to be included.

In [17, 18], it has been proved that on the $U(5)$–$O(6)$ transition leg there exists a critical point for a second-order phase transition, while the $U(5)$–$SU(3)$ leg has a first-order phase transition. Actually, the first-order phase transition takes place not only on the mentioned leg of the Casten's triangle, but covers all the interior of the triangle up to the second order [19]. Examples of such nuclei, falling inside the triangle, are the Os isotopes [20].

Recently, Iachello [21, 22] pointed out that these critical points correspond to distinct symmetries, namely $E(5)$ and $X(5)$, respectively. For the critical value of an ordering parameter, energies are given by the zeros of a Bessel function of half-integer and irrational indices, respectively.

The description of low lying states in terms of Bessel functions was used first by Jean and Willet [13], but the interesting feature saying that this is a critical picture in a phase transition and defines a new symmetry was indeed advanced first in [21].

Representatives for the two symmetries have been experimentally identified. To give an example, the relevant data for ^{134}Ba [23] and ^{152}Sm [24] suggest that they are close to the $E(5)$ and $X(5)$ symmetries, respectively. Another candidate for $E(5)$ symmetry is ^{102}Pd [25, 27]. A systematic search for $E(5)$ behavior in nuclei has been reported in [26].

In [30], we advanced the hypothesis that the critical point in a phase transition is state dependent. We tested this with a hybrid model for ^{134}Ba and ^{104}Ru. A similar property of the phase transition was investigated in the context of a schematic two-level model in [31, 32]. A rigorous analysis of the characteristics of excited state quantum phase transitions is performed in [33].

The departure from the γ unstable picture has been treated by several authors [28] whose contributions are reviewed by Fortunato in [34]. The difficulty in treating the γ degree of freedom consists in the fact that this variable is coupled to the rotation variables. A full solution for the Bohr–Mottelson Hamiltonian including an explicit treatment of γ deformation variable can be found in [35–39]. Therein, we treated separately also the γ unstable and the rotor Hamiltonian. A more complete study of the rotor Hamiltonian and the distinct phases associated with a tilted moving rotor is given in [40].

The treatment of the γ variable becomes even more complicated when we add to the liquid drop Hamiltonian a potential depending on β and γ at a time. To simplify the starting problem related to the inclusion of the γ variable, one uses model potentials which are sums of a beta and a γ depending potentials. In this way, the nice feature for the beta variable to be decoupled from the remaining four variables, specific to the harmonic liquid drop, is preserved. Further, the potential in γ is expanded either around to $\gamma = 0$ or around $\gamma = \frac{\pi}{6}$. In the first case, if only the singular term is retained, one obtains the infinite square well (ISW) model described by Bessel functions in gamma. If the γ^2 term is added to this term, then the Laguerre functions are the eigenstates of the approximated gamma depending Hamiltonian, which results in defining the functions characterizing the $X(5)$ approach.

The drawback of these approximation consists in that the resulting γ depending functions are not periodic as the starting Hamiltonian is. Moreover, they are orthonormalized on unbound intervals although the underlying equation was derived under the condition of $|\gamma|$ small. The scalar product of the space of the resulting functions is not defined based on the measure $|\sin 3\gamma| \mathrm{d}\gamma$ as happens in the liquid drop model. Under these circumstances it happens that the approximated Hamiltonian in γ looses its hermiticity.

In some earlier publications [41, 42], we proposed a scheme where the gamma variable is described by a solvable Hamiltonian whose eigenstates are spheroidal functions which are periodic. Here, we give details about the calculations and describe some new numerical applications. Moreover, the formalism was completed by treating the β variable by a Schrödinger equation associated with the Davidson potential. Alternatively, we considered the equation for a five-dimensional square well potential. We have shown that the new treatment of the gamma variable removes the drawbacks mentioned above and moreover brings a substantial improvement of the numerical analysis.

Here, we keep the description of the gamma variable by spheroidal functions and use a new potential for the beta variable which seems to be more suitable for a realistic description of more complex spectra. We call this approach as sextic and spheroidal approach (SSA). The potential is that of a sextic oscillator plus a centrifugal term which leads to a quasi-exactly solvable model. The resulting formalism will be applied to ten nuclei which were not included in our previous descriptions and moreover are suspected to be good candidate for exhibiting $X(5)$ features having the ratio of excitation energies of the ground band members 4^+ and 2^+ close to the value of 2.9. The results of our calculations are compared with those obtained through other methods such as the ISW, D and CSM.

The goals presented in the previous section will be developed according to the following plan. In section 2, the main ingredients of the theoretical models $X(5)$, ISW, D and SSA will be briefly presented. The CSM is separately described in section 3. Numerical results are given and commented in section 4, while the final conclusions are drawn in section 5.

2. The separation of variables and solutions

In order to describe the critical nuclei of the $U(5)$–$SU(3)$ shape phase transition, we resort the Bohr–Mottelson Hamiltonian with a potential depending on both the β and γ variables:

$$H\psi(\beta,\gamma,\Omega)=E\psi(\beta,\gamma,\Omega), \tag{2.1}$$

where

$$H=-\frac{\hbar^2}{2B}\left[\frac{1}{\beta^4}\frac{\partial}{\partial\beta}\beta^4\frac{\partial}{\partial\beta}+\frac{1}{\beta^2\sin 3\gamma}\frac{\partial}{\partial\gamma}\sin 3\gamma\frac{\partial}{\partial\gamma}-\frac{1}{4\beta^2}\sum_{k=1}^{3}\frac{\hat{Q}_k^2}{\sin^2\left(\gamma-\frac{2\pi}{3}k\right)}\right]+V(\beta,\gamma). \tag{2.2}$$

Here, β and γ are the intrinsic deformation variables, Ω denotes the Euler angles θ_1, θ_2 and θ_3, $\hat{Q}_k$ are the angular momentum components in the intrinsic reference frame, while B is the so-called mass parameter.

2.1. The separation of variables

To achieve the separation of variables in equation (2.1), some approximations are necessary. Choosing the potential energy in the form [13, 34]

$$V(\beta,\gamma)=V_1(\beta)+\frac{V_2(\gamma)}{\beta^2}, \tag{2.3}$$

the β variable is separated from the γ and the Euler angles Ω, which are still coupled due to the rotational term:

$$W=\frac{1}{4}\sum_{k=1}^{3}\frac{\hat{Q}_k^2}{\sin^2\left(\gamma-\frac{2\pi}{3}k\right)}. \tag{2.4}$$

Furthermore, the γ is separated from the Euler angles by using the second-order power expansion of the rotational term around the equilibrium value $\gamma_0=0^0$ (see equation (B.5) from [42]):

$$W\approx\frac{1}{3}\hat{Q}^2+\left(\frac{1}{4\sin^2\gamma}-\frac{1}{3}\right)\hat{Q}_3^2+\frac{2}{2\sqrt{3}}(\hat{Q}_2^2-\hat{Q}_1^2)\gamma+\frac{2}{3}(\hat{Q}^2-\hat{Q}_3^2)\gamma^2+\mathcal{O}(\gamma^3), \tag{2.5}$$

and then averaging the result with the Wigner function $D^{(L)}_{M,K}$:

$$\langle W\rangle=\frac{1}{3}L(L+1)+\left(\frac{1}{4\sin^2\gamma}-\frac{1}{3}\right)K^2+\frac{2}{3}[L(L+1)-K^2]\gamma^2. \tag{2.6}$$

The term $L(L+1)/3$ multiplied by $1/\beta^2$ is transferred to the equation for β,

$$\left[-\frac{1}{\beta^4}\frac{\partial}{\partial\beta}\beta^4\frac{\partial}{\partial\beta}+\frac{L(L+1)}{3\beta^2}+v_1(\beta)\right]f(\beta)=\varepsilon_\beta f(\beta), \tag{2.7}$$

while the sum of remaining terms, denoted with $\tilde{V}(\gamma,L,K)$, is kept in the equation for γ:

$$\left[-\frac{1}{\sin 3\gamma}\frac{\partial}{\partial\gamma}\sin 3\gamma\frac{\partial}{\partial\gamma}+\tilde{V}(\gamma,L,K)+v_2(\gamma)\right]\eta(\gamma)=\tilde{\varepsilon}_\gamma\eta(\gamma). \tag{2.8}$$

In equations (2.7) and (2.8), the following notations were used:

$$v_1(\beta) = \frac{2B}{\hbar^2}V_1(\beta), \quad v_2(\gamma) = \frac{2B}{\hbar^2}V_2(\gamma), \quad \varepsilon_\beta = \frac{2B}{\hbar^2}E_\beta, \quad \tilde{\varepsilon}_\gamma = \langle\beta^2\rangle\frac{2B}{\hbar^2}E_\gamma. \tag{2.9}$$

Equations (2.7) and (2.8) are to be separately solved and finally the full solution of equation (2.1) is obtained by combining the contributions coming from each variable. In what follows, we shall give the necessary details for solving the above-mentioned equations.

2.2. Solutions of the β equation

Solutions of the β equation, corresponding to different potentials, were considered by several authors [34, 43]. Here, we mention only three of them, namely the ISW, the Davidson and the sextic potentials. Details about how to solve the β equation for these potentials can be found in [42, 44].

2.2.1. The infinite square well potential. The solution of the β equation with an ISW potential, having the expression

$$v_1(\beta) = \begin{cases} 0, & \beta \leqslant \beta_\omega \\ \infty, & \beta > \beta_\omega \end{cases}, \tag{2.10}$$

was first time given in [13] and then in [21, 22] for $E(5)$ and $X(5)$ models. The β wavefunctions are written in terms of the Bessel functions of half-integer [21] and irrational indices [22], respectively. The solution for $X(5)$ is

$$f_{s,L}(\beta) = C_{s,L}\beta^{-\frac{3}{2}}J_\nu\left(\frac{x_{s,L}}{\beta_\omega}\beta\right), \quad \nu = \sqrt{\frac{L(L+1)}{3} + \frac{9}{4}}, \quad s = 1, 2, 3, \ldots. \tag{2.11}$$

Here, $C_{s,L}$ is the normalization factor, which is determined from the condition

$$\int_0^{\beta_\omega} (f_{s,L}(\beta))^2\beta^4\,\mathrm{d}\beta = 1. \tag{2.12}$$

The corresponding eigenvalues are given in terms of the Bessel zeros $x_{s,L}$:

$$E_\beta(s, L) = \frac{\hbar^2}{2B}\left(\frac{x_{s,L}}{\beta_\omega}\right)^2. \tag{2.13}$$

2.2.2. The Davidson potential. Choosing in equation (2.7) a Davidson potential [29] of the form

$$v_1(\beta) = \beta^2 + \frac{\beta_0^4}{\beta^2}, \tag{2.14}$$

solutions are the generalized Laguerre polynomials:

$$f_{n_\beta,m_\beta}(\beta) = \sqrt{\frac{2n_\beta!}{\Gamma(n_\beta + m_\beta + 1)}}L_{n_\beta}^{m_\beta}(\beta^2)\beta^{m_\beta-\frac{3}{2}}\,\mathrm{e}^{-\frac{\beta^2}{2}}, \quad m_\beta = \sqrt{\frac{L(L+1)}{3} + \frac{9}{4} + \beta_0^4}. \tag{2.15}$$

The wavefunctions, $f_{n_\beta,m_\beta}(\beta)$, are normalized to unity with the integration measure $\beta^4\,\mathrm{d}\beta$. Energies have the following expression:

$$E_\beta(n_\beta, L) = \frac{\hbar^2}{2B}\left(2n_\beta + 1 + \sqrt{\frac{L(L+1)}{3} + \frac{9}{4} + \beta_0^4}\right), \quad n_\beta = 0, 1, 2, \ldots, \quad n_\beta = s - 1. \tag{2.16}$$

2.2.3. The sextic oscillator potential with a centrifugal barrier. The solution of the β equation with a sextic potential, for critical nuclei of the $U(5)\rightarrow SU(3)$ shape phase transition, was obtained by taking into consideration the solution of the Schrödinger equation with a sextic potential given in [45] and applied to the $E(5)$ like nuclei in [46] and to the triaxial nuclei in [44].

In order to reduce the β equation to the Schrödinger equation with a sextic potential [45], we rewrite the averaged rotational term, given by equation (2.6), in the following form:

$$\langle W\rangle = [L(L+1)-2] + \left[2-\frac{2}{3}L(L+1)\right] + \left(\frac{1}{4\sin^2\gamma}-\frac{1}{3}\right)K^2 + \frac{2}{3}[L(L+1)-K^2]\gamma^2. \tag{2.17}$$

As already mentioned, the first term of the above equation is added to the β equation, while the other terms remain in the γ equation. Making the substitution $f(\beta)=\beta^{-2}\varphi(\beta)$, we have

$$\left[-\frac{\partial^2}{\partial\beta^2}+\frac{L(L+1)}{\beta^2}+v_1(\beta)\right]\varphi(\beta)=\varepsilon_\beta\varphi(\beta). \tag{2.18}$$

The sextic potential is chosen such that to obtain the description from [44]:

$$v_1^{\pm}(\beta)=(b^2-4ac^{\pm})\beta^2+2ab\beta^4+a^2\beta^6+u_0^{\pm},\quad c^{\pm}=\frac{L}{2}+\frac{5}{4}+M. \tag{2.19}$$

Here, c is a constant which has two different values, one for L even and other for L odd:

$$(M,L):(k,0);(k-1,2);(k-2,4);(k-3,6)\ldots\Rightarrow c=k+\tfrac{5}{4}\equiv c^{+}(L\text{-even}), \tag{2.20}$$

$$(M,L):(k,1);(k-1,3);(k-2,5);(k-3,7)\ldots\Rightarrow c=k+\tfrac{7}{4}\equiv c^{-}(L\text{-odd}). \tag{2.21}$$

The constants $u_0^{\pm}$ are fixed such that the potential for L odd has the same minimum energy as the potential for L even. The solutions of equation (2.18), with the potential given by equation (2.19), are

$$\varphi^{(M)}_{n_\beta,L}(\beta)=N_{n_\beta,L}P^{(M)}_{n_\beta,L}(\beta^2)\beta^{L+1}\,\mathrm{e}^{-\frac{a}{4}\beta^4-\frac{b}{2}\beta^2},\quad n_\beta=0,1,2,\ldots M, \tag{2.22}$$

where $N_{n_\beta,L}$ are the normalization factor, while $P^{(M)}_{n_\beta,L}(\beta^2)$ are polynomials in x^2 of n_β order. The corresponding excitation energy is

$$E_\beta(n_\beta,L)=\frac{\hbar^2}{2B}\left[b(2L+3)+\lambda^{(M)}_{n_\beta}(L)+u_0^{\pm}\right],\quad n_\beta=0,\quad 1,2,\ldots,M, \tag{2.23}$$

where $\lambda^{(M)}_{n_\beta}=\varepsilon_\beta-u_0^{\pm}-4bs$ is the eigenvalue of the equation:

$$\left[-\left(\frac{\partial^2}{\partial\beta^2}+\frac{4s-1}{\beta}\frac{\partial}{\partial\beta}\right)+2b\beta\frac{\partial}{\partial\beta}+2a\beta^2\left(\beta\frac{\partial}{\partial\beta}-2M\right)\right]P^{(M)}_{n_\beta,L}(\beta^2)=\lambda^{(M)}_{n_\beta}P^{(M)}_{n_\beta,L}(\beta^2). \tag{2.24}$$

2.3. Solutions of the γ equation

2.3.1. The X(5) model. Within the $X(5)$model [22], devoted to the description of the critical point in the phase transition $SU(5)\rightarrow SU(3)$, the potential is a sum of an ISW in the β variable and a harmonic oscillator in the γ variable. For the rotational term and the other terms of the γ equation, the first-order Taylor expansion around $\gamma_0=0^0$ is considered, which results in obtaining for the γ variable the radial equation of a two-dimensional oscillator with the solution

$$\eta_{n_\gamma,K}(\gamma)=C_{n,K}\gamma^{|K/2|}\,\mathrm{e}^{-(3a)\gamma^2/2}L_n^{|K|}(3a\gamma^2),\quad n=\left(\frac{n_\gamma-|K|}{2}\right), \tag{2.25}$$

Table 1. The fitted values of the parameters involved in the expressions of the energies and transition probabilities of the $X(5)$ model are given for each considered nucleus.

$X(5)$	^{176}Os	^{178}Os	^{180}Os	^{188}Os	^{190}Os	^{150}Nd	^{156}Dy	^{166}Hf	^{168}Hf	^{170}W
B_1 (keV)	18.08	18.13	18.79	25.56	26.92	17.77	17.02	23.46	20.14	20.68
X (keV)	822.28	818.68	880.10	452.71	438.53	966.50	950.46	698.15	770.26	799.14
t $[W.u.]^{1/2}$	1.29	1.22	0.84	0.86	0.76	1.03	1.19	0.99	1.19	0.89
t' $[W.u.]^{1/2}$	–	–	–	0.92	1.19	0.49	0.81	–	–	–

where $L_n^{|K|}$ are the generalized Laguerre polynomials. The eigenvalue of the γ equation has the following expression:

$$\varepsilon_\gamma = \frac{3a}{\sqrt{\langle\beta^2\rangle}}(n_\gamma + 1) - \frac{(K/2)^2}{\langle\beta^2\rangle}\frac{4}{3}, \tag{2.26}$$

where a is a parameter characterizing the oscillator potential in the γ variable. The total energy and wavefunction are obtained by combining the results of all variables:

$$E(s, L, n_\gamma, K) = E_0 + B_1(x_{s,L})^2 + An_\gamma + CK^2, \tag{2.27}$$

$$\Psi(\beta, \gamma, \Omega) = \frac{1}{\sqrt{2(1+\delta_{K,0})}} f_{s,L}(\beta)\left[\eta_{n_\gamma,K}(\gamma)D^L_{M,K}(\Omega) + (-1)^{L+K}\eta_{n_\gamma,-K}(\gamma)D^L_{M,-K}(\Omega)\right]. \tag{2.28}$$

If the total energy (2.27) is normalized to the energy of the ground state, then we will have for the ground band and for the first beta band the expression

$$E(s, L, 0, 0) - E(1, 0, 0, 0) = B_1\left(x^2_{s,L} - x^2_{1,0}\right), \quad s = 1, \quad 2; \quad L = 0, 2, 4, 6, \ldots, \tag{2.29}$$

while for the first γ band

$$E(s, L, 1, 2) - E(1, 0, 0, 0) = B_1\left(x^2_{1,L} - x^2_{1,0}\right) + A + 4C, \quad L = 2, 3, 4, 5, \ldots. \tag{2.30}$$

One notes that the parameters A and C give contribution only to the γ band energies, and that these two parameters can be replaced with only one parameter, for example $X = A + 4C$. The total energy for the ground band and for the first β and γ bands, normalized to the energy of the ground state, can be written in the following form:

$$E(s, L, n_\gamma, K) - E(1, 0, 0, 0) = B_1\left(x^2_{s,L} - x^2_{1,0}\right) + \delta_{K,2}X. \tag{2.31}$$

Further, the parameters B_1 and X will be fitted by the least-squares procedure for each considered nucleus.

2.3.2. The ISW model. Within the ISW model, employed in this paper, the β equation is treated as in the $X(5)$ model, using an ISW, while the γ equation is reduced to a spheroidal equation. The ISW model was proposed by one of the authors (AAR) and his collaborators in [41] and subsequently with more details and applications in [42]. Here, only the solutions will be presented. The potential $v_2(\gamma)$ was chosen such that a minimum in $\gamma = 0^0$ is achieved:

$$v_2(\gamma) = u_1 \cos 3\gamma + u_2 \cos^2 3\gamma. \tag{2.32}$$

This potential is renormalized by a contribution coming from the γ rotational term and consequently an effective reduced potential for the γ variable results

$$\tilde{v}_2(\gamma) = u_1 \cos 3\gamma + u_2 \cos^2 3\gamma + \frac{9}{4\sin^3 3\gamma}, \tag{2.33}$$

Table 2. The same as in table 1, but for the ISW model.

ISW	^{176}Os	^{178}Os	^{180}Os	^{188}Os	^{190}Os	^{150}Nd	^{156}Dy	^{166}Hf	^{168}Hf	^{170}W
B_1 (keV)	14.30	14.54	13.21	25.50	21.83	14.68	11.43	23.31	19.12	14.87
F (keV)	24.24	23.19	44.66	0.69	36.73	28.88	45.99	1.69	11.30	41.12
u_1	−159.24	−168.08	−36.729	−25 000	−4999.35	−152.35	−12.55	−10 000	−385.35	−44.36
u_2	0	0	0	0	2560.22	0	0	0	0	0
t_1 $[W.u.]^{1/2}$	−52.91	473.53	3302.3	503.11	419.67	538.99	591.54	1881.39	1197.94	1827.11
t_2 $[W.u.]^{1/2}$	−4305.14	−1323.6	14 304.2	−241.19	−48.09	−387.08	−468.57	8242.45	2702.98	6436.57

Table 3. The same as in table 1, but for the D model.

D	^{176}Os	^{178}Os	^{180}Os	^{188}Os	^{190}Os	^{150}Nd	^{156}Dy	^{166}Hf	^{168}Hf	^{170}W
E (keV)	316.34	317.31	334.32	559.76	462.44	369.50	324.08	532.22	463.88	379.93
F (keV)	38.41	37.33	39.01	28.48	42.45	26.48	33.11	11.87	25.87	37.72
β_0	1.64	1.56	1.61	1.98	1.64	1.71	1.45	1.79	2.02	1.63
u_1	−55.48	−57.20	−52.40	−7.70	−4098.61	−168.78	−58.16	−320.01	−130.49	−54.50
u_2	0	0	0	0	2167.18	0	0	0	0	0
t_1 $[W.u.]^{1/2}$	197.92	264.47	758.41	126.88	126.70	154.70	191.28	448.76	329.01	411.63
t_2 $[W.u.]^{1/2}$	−25.31	78.30	931.21	−17.09	−3.92	−25.31	−13.46	430.42	193.06	363.66

Table 4. The same as in table 1, but for the SSA model.

SSA	^{176}Os	^{178}Os	^{180}Os	^{188}Os	^{190}Os	^{150}Nd	^{156}Dy	^{166}Hf	^{168}Hf	^{170}W
E (keV)	0.99	0.46	1.46	2.53	5.29	0.75	0.91	1.82	0.54	0.31
F (keV)	2.67	3.12	1.69	11.31	5.55	3.87	1.93	15.97	1.99	2.84
a	951.49	4466.56	600.70	644.98	111.79	2636.48	1248.40	1205.13	7897.62	13197.99
b	126	279	50	27	15.8	88	87	46	32	341
u_1	−5607.45	−4048.06	−15 000	−215.19	−452.74	−3877.84	−10 000	−224.90	−9980.01	−4585.44
u_2	0	0	0	0	0	0	0	0	0	0
t_1 $[W.u.]^{1/2}$	376.70	2260.6	8541.32	1033.43	675.12	1754.26	1882.91	4759.23	3463.05	8901.59
t_2 $[W.u.]^{1/2}$	−32 619.3	−22 343.8	117781	−1022.41	32.73	−6698.41	−4846.17	46 113.3	15 247.9	200 989

Table 5. The same as in table 1, but for the CSM model.

CSM	^{176}Os	^{178}Os	^{180}Os	^{188}Os	^{190}Os	^{150}Nd	^{156}Dy	^{166}Hf	^{168}Hf	^{170}W
A_1 (keV)	17.03	17.26	16.51	10.25	9.063	19.219	15.45	14.87	16.04	16.19
A_2 (keV)	4.33	4.32	5.19	14.40	15.68	3.467	5.2	7.13	6.40	6.018
A_3 (keV)	−395.96	−240.13	−7.39	101.362	6.84	−658.299	−559.913	−5.04	−61.47	−186.946
A_4 (keV)	−275.24	−158.87	13.83	0.0	0.0	−491.884	−398.775	0.0	−36.48	−124.55
A_5 (keV)	−4.93	30.76	80.01	0.0	0.0	−438.394	−32.15	0.0	0.0	0.0
d	2.33	2.36	2.26	2.35	2.05	2.42	2.1	2.08	2.43	2.14
q_1 $[W.u.]^{1/2}$	0.411	0.246	0.86	0.409	0.229	0.527	1.112	0.158	0.211	–0.217
q_2 $[W.u.]^{1/2}$	−3.698	−3.862	6.99	0.785	1.213	−4.916	−9.474	−5.075	−3.936	−5.602
q_3 $[W.u.]^{1/2}$	0.0	0.0	0.0	−5.222	−9.395	6.344	19.576	0.0	0.0	0.0

Table 6. The energy spectra of the ground and first β and γ bands of the ^{176}Os nucleus yielded by the $X(5)$, ISW, D, SSA and CSM models are compared with the corresponding experimental data taken from [53]. The energies are given in keV units. The approach which describe best the experimental data is mentioned in a box.

^{176}Os	Exp.	$X(5)$	ISW	D	SSA	CSM
2^+_g	135	126	115	125	125	135
4^+_g	396	367	340	386	377	394
6^+_g	743	686	647	746	723	742
8^+_g	1158	1072	1026	1176	1143	1159
10^+_g	1634	1520	1473	1661	1624	1631
12^+_g	2168	2028	1986	2192	2157	2152
14^+_g	2755	2593	2564	2764	2736	2718
16^+_g	3382	3216	3205	3374	3354	3326
18^+_g	4019	3894	3909	4017	4008	3973
20^+_g	4683	4628	4673	4693	4695	4660
22^+_g	5399	5417	5499	5399	5412	5385
24^+_g	6147	6261	6385	6134	6157	6147
0^+_β	601	714	565	633	498	601
2^+_β	742	942	760	757	723	742
4^+_β	1026	1351	1118	1019	1075	1032
6^+_β	1432	1865	1578	1378	1511	1432
8^+_β		2458	2121	1808	2011	1914
10^+_β		3121	2738	2293	2565	2411
2^+_γ	864	949	951	926	943	989
3^+_γ	1038	1058	1056	1045	1053	1081
4^+_γ	1224	1189	1184	1196	1195	1201
5^+_γ	1410	1340	1333	1371	1345	1342
6^+_γ		1509	1503	1568	1542	1511
7^+_γ		1694	1691	1784	1719	1689
8^+_γ		1895	1898	2016	1962	1900
9^+_γ		2111	2124	2264	2161	2106
10^+_γ		2343	2367	2525	2444	2354
rms (keV)		156	119	25	41	39

whose minima are shifted with respect to the $v_2(\gamma)$ minima. This can be viewed as the reduced potential of

$$\tilde{V}_2 = \frac{\hbar^2}{2B}\tilde{v}_2. \tag{2.34}$$

Performing a second-order expansion in $\sin 3\gamma$ of $v_2(\gamma)$ and of the terms originating from the rotational term, i.e. $\frac{9}{4\sin^3 3\gamma}$, and then making the change of variable $x = \cos 3\gamma$ in equation (2.8), we obtain the equation for the spheroidal functions [42]:

$$\left[(1-x^2)\frac{\partial^2}{\partial x^2} - 2x\frac{\partial}{\partial x} + \lambda_{m_\gamma,n_\gamma} - c^2x^2 - \frac{m_\gamma^2}{1-x^2}\right] S_{m_\gamma,n_\gamma}(x) = 0, \tag{2.35}$$

Table 7. The same as in table 6, but for ^{178}Os. The experimental data are taken from [57].

^{178}Os	Exp.	$X(5)$	ISW	D	SSA	CSM
2^+_g	132	127	116	131	130	132
4^+_g	399	368	342	402	388	389
6^+_g	762	688	650	769	739	736
8^+_g	1194	1075	1031	1203	1163	1152
10^+_g	1682	1525	1479	1689	1647	1625
12^+_g	2220	2033	1994	2220	2181	2147
14^+_g	2805	2600	2572	2789	2758	2715
16^+_g	3429	3224	3214	3395	3374	3325
18^+_g	4020	3905	3918	4033	4025	3975
20^+_g	4663	4641	4684	4701	4706	4664
22^+_g	5382	5432	5510	5399	5415	5391
24^+_g	6155	6278	6397	6125	6150	6155
0^+_β	651	716	574	635	493	651
2^+_β	771	944	771	766	730	771
4^+_β	1023	1355	1133	1037	1092	1029
6^+_β	1396	1870	1598	1403	1535	1396
8^+_β		2464	2144	1838	2041	1850
10^+_β		3129	2766	2324	2599	2374
2^+_γ	864	945	947	916	936	999
3^+_γ	1032	1055	1052	1041	1048	1091
4^+_γ	1213	1187	1181	1195	1195	1211
5^+_γ	1416	1338	1331	1375	1346	1350
6^+_γ		1507	1501	1575	1546	1519
7^+_γ		1692	1690	1793	1725	1696
8^+_γ		1894	1898	2027	1971	1907
9^+_γ		2111	2123	2275	2170	2113
10^+_γ		2343	2367	2537	2455	2361
rms (keV)		170	141	22	61	54

where

$$\lambda_{m_\gamma,n_\gamma} = \frac{1}{9}\left[\tilde{\varepsilon}_\gamma - \frac{u_1}{2} - \frac{11}{27}D + \frac{1}{3}L(L+1)\right],$$
$$c^2 = \frac{1}{9}\left(\frac{u_1}{2} + u_2 - \frac{2}{27}D\right),$$
$$m_\gamma = \frac{K}{2}, \quad D = L(L+1) - K^2 - 2. \tag{2.36}$$

From equation (2.36), we can determine the eigenvalue of the γ equation:

$$E_\gamma(n_\gamma, m_\gamma, L, K) = \frac{1}{\langle\beta^2\rangle}\frac{\hbar^2}{2B}\left(9\lambda_{m_\gamma,n_\gamma}(c) + \frac{u_1}{2} + \frac{11}{27}D - \frac{L(L+1)}{3}\right). \tag{2.37}$$

In equation (2.37), the term $u_1/2$ is washed out when the total energy is normalized to the ground state energy, which results in obtaining the γ eigenvalue depending on the sum of the γ potential parameters, due to the term c^2. Hence, in some cases we can set one parameter to be equal to zero, for example u_2, and consequently fit only u_1. The γ functions are normalized to unity with the integration measure $|\sin 3\gamma|\,\mathrm{d}\gamma$ as the Bohr–Mottelson model requires

$$\frac{3(2n_\gamma+1)(n_\gamma-m_\gamma)!}{2(n_\gamma+m_\gamma)!}\int_0^{\frac{\pi}{3}} |S_{m_\gamma,n_\gamma}(\cos 3\gamma)|^2 |\sin 3\gamma|\,\mathrm{d}\gamma = 1. \tag{2.38}$$

Table 8. The same as in table 6, but for ^{180}Os. The experimental data are taken from [58].

^{180}Os	Exp.	$X(5)$	ISW	D	SSA	CSM
2^+_g	132	131	124	133	125	147
4^+_g	409	381	374	412	384	423
6^+_g	795	713	723	792	748	792
8^+_g	1257	1115	1163	1244	1196	1234
10^+_g	1768	1580	1688	1752	1716	1735
12^+_g	2309	2108	2297	2308	2299	2291
14^+_g	2875	2695	2987	2906	2937	2897
0^+_β	736	742	522	669	555	736
2^+_β	831	979	720	802	774	831
4^+_β	1053	1404	1093	1080	1137	1051
6^+_β	1379	1938	1584	1460	1596	1379
8^+_β		2554	2175	1912	2133	1799
10^+_β		3243	2858	2421	2734	2299
2^+_γ	870	1011	975	935	985	969
3^+_γ	1023	1125	1090	1062	1100	1068
4^+_γ	1197	1262	1233	1221	1245	1198
5^+_γ	1406	1418	1402	1406	1402	1348
6^+_γ	1627	1593	1596	1614	1609	1529
7^+_γ	1881	1786	1813	1841	1797	1718
8^+_γ		1995	2054	2084	2057	1944
9^+_γ	2411	2220	2318	2344	2270	2164
10^+_γ		2460	2604	2617	2577	2429
rms (keV)		194	96	38	92	35

The total energy is obtained by summing the contributions coming from the β (2.13) and the γ (2.37) equations:

$$E(s, n_\gamma, m_\gamma, L, K) = B_1 x^2_{s,L} + F\left[9\lambda_{m_\gamma,n_\gamma}(c) + \frac{u_1}{2} + \frac{11}{27}D - \frac{L(L+1)}{3}\right], \tag{2.39}$$

where the following notations were introduced:

$$B_1 = \frac{1}{\beta^2_\omega}\frac{\hbar^2}{2B}, \quad F = \frac{1}{\langle\beta^2\rangle}\frac{\hbar^2}{2B}. \tag{2.40}$$

The total wavefunction is

$$\Psi(\beta, \gamma, \Omega) = C_{s,L}C_{n_\gamma,m_\gamma}C_{L,K}\beta^{-\frac{3}{2}}J_\nu\left(\frac{x_{s,L}}{\beta_\omega}\beta\right)S_{m_\gamma,n_\gamma}(\cos 3\gamma)\left[D^L_{M,K}(\Omega) + (-1)^L D^L_{M,-K}(\Omega)\right], \tag{2.41}$$

where with C_{n_γ,m_γ} was denoted the normalization factor of the γ function, while $C_{L,K}$ is the normalization factor of the Wigner function:

$$C_{L,K} = \sqrt{\frac{2L+1}{16\pi^2(1+\delta_{K,0})}}. \tag{2.42}$$

2.3.3. The D model. The D model was proposed by the present authors and collaborators in [42] and differs from the ISW model by that the ISW potential for the β variable is replaced

Table 9. The same as in table 6, but for ^{188}Os. The experimental data are taken from [59].

^{188}Os	Exp.	$X(5)$	ISW	D	SSA	CSM
2_g^+	155	179	179	151	152	150
4_g^+	478	519	519	479	476	468
6_g^+	940	970	970	945	935	934
8_g^+	1515	1516	1516	1512	1501	1535
10_g^+	2170	2149	2150	2156	2154	2264
12_g^+	2856	2867	2868	2860	2877	3116
0_β^+	1086	1009	1007	1120	1063	1164
2_β^+	1305	1331	1328	1270	1330	1305
4_β^+		1910	1907	1599	1808	1621
6_β^+		2636	2632	2064	2421	2096
8_β^+		3474	3470	2632	3132	2717
10_β^+		4412	4407	3276	3920	3475
2_γ^+	633	631	631	627	641	665
3_γ^+	790	786	785	773	791	790
4_γ^+	966	972	971	959	969	956
5_γ^+	1181	1185	1185	1180	1172	1157
6_γ^+	1425	1423	1423	1432	1434	1399
7_γ^+	1686	1685	1684	1709	1674	1669
8_γ^+		1969	1969	2009	2008	1983
9_γ^+		2275	2275	2329	2273	2318
10_γ^+		2602	2603	2666	2670	2701
rms (keV)		27	27	16	13	36

with the Davidson potential (2.14). Hence, the total energy of the system is obtained by adding the energy of the β equation with the Davidson potential given by equation (2.16) and the energy of the γ equation (2.37):

$$E(n_\beta, n_\gamma, m_\gamma, L, K) = E\left(2n_\beta + 1 + \sqrt{\frac{L(L+1)}{3} + \frac{9}{4} + \beta_0^4}\right) + F\left[9\lambda_{m_\beta, n_\gamma}(c) + \frac{u_1}{2} + \frac{11}{27}D - \frac{L(L+1)}{3}\right], \quad (2.43)$$

where $E = \hbar^2/2B$. The total wavefunction has the expression

$$\Psi(\beta, \gamma, \Omega) = C_{n_\beta, L} C_{n_\gamma, m_\gamma} C_{L,K} f_{n_\beta, L}(\beta) S_{m_\gamma, n_\gamma}(\cos 3\gamma)\left[D^L_{M,K}(\Omega) + (-1)^L D^L_{M,-K}(\Omega)\right], \quad (2.44)$$

where $C_{n_\beta, L}$ is the normalization factor of $f_{n_\beta, L}(\beta)$ given by equation (2.15).

2.3.4. The present approach. In the present approach, called conventionally the SSA, a sextic potential (2.19) for the β variable is considered, while for the γ variable a periodic potential (2.32) with a minimum at $\gamma_0 = 0^0$. The β equation is quasi-exactly solved, having the solutions given by equations (2.22) and (2.23), while the γ equation is reduced to the spheroidal equation (2.35) with

$$\lambda_{m_\gamma, n_\gamma} = \frac{1}{9}\left[\tilde{\varepsilon}_\gamma - \frac{u_1}{2} - \frac{11}{27}D + \frac{1}{3}L(L+1)\right] + \frac{2L(L+1)}{27},$$
$$c^2 = \frac{1}{9}\left(\frac{u_1}{2} + u_2 - \frac{2}{27}D\right),$$
$$m_\gamma = \frac{K}{2}, \quad D = L(L+1) - K^2 - 2. \quad (2.45)$$

Table 10. The same as in table 6, but for ^{190}Os. The experimental data are taken from [60].

^{190}Os	Exp.	$X(5)$	ISW	D	SSA	CSM
2_g^+	187	188	182	178	172	180
4_g^+	548	547	541	551	531	531
6_g^+	1050	1022	1034	1062	1034	1031
8_g^+	1666	1597	1647	1672	1653	1670
10_g^+	2357	2264	2373	2359	2367	2441
0_β^+	912	1063	862	925	860	912
2_β^+	1115	1402	1166	1103	1168	1072
4_β^+		2012	1729	1476	1682	1417
6_β^+		2777	2457	1987	2331	1925
8_β^+		3659	3319	2596	3083	2582
10_β^+		4647	4305	3283	3921	3380
2_γ^+	558	627	594	583	593	618
3_γ^+	756	789	756	750	754	756
4_γ^+	955	985	955	957	954	939
5_γ^+	1204	1210	1187	1199	1172	1156
6_γ^+	1474	1461	1451	1469	1459	1419
7_γ^+		1736	1745	1764	1718	1708
8_γ^+	2090	2035	2067	2081	2080	2045
9_γ^+		2358	2419	2417	2370	2401
10_γ^+	2772	2702	2799	2770	2798	2810
rms (keV)		98	26	10	27	36

In equation (2.45), the term $2L(L+1)/3$ multiplied with $1/9$ comes from the rotational term (2.17). The expression for the total energy of the system is obtained by using equations (2.23) and (2.45):

$$E(n_\beta, n_\gamma, m_\gamma, L, K) = E\left[b(2L+3) + \lambda_{n_\beta}^{(M)} + u_0^{\pm}\right] + F\left[9\lambda_{m_\beta,n_\gamma}(c) + \frac{u_1}{2} + \frac{11}{27}D - L(L+1)\right]. \tag{2.46}$$

The corresponding wavefunction is

$$\Psi(\beta, \gamma, \Omega) = N_{n_\beta,L} C_{n_\gamma,m_\gamma} C_{L,K} \beta^{-2} \varphi_{n_\beta,L}(\beta) S_{m_\gamma,n_\gamma}(\cos 3\gamma)\left[D^L_{M,K}(\Omega) + (-1)^L D^L_{M,-K}(\Omega)\right], \tag{2.47}$$

where $\varphi_{n_\beta,L}(\beta)$ is given by equation (2.22).

2.4. E2 transition probabilities

The reduced $E2$ transition probabilities are determined by

$$B(E2; L_i \to L_f) = |\langle L_i || T_2^{(E2)} || L_f \rangle|^2, \tag{2.48}$$

where the Rose convention [47] was used. For the ISW, D and SSA models, in equation (2.48), an anharmonic transition operator is used:

$$T_{2\mu}^{(E2)} = t_1 \beta \left[\cos\gamma D^2_{\mu 0}(\Omega) + \frac{\sin\gamma}{\sqrt{2}}\left(D^2_{\mu 2}(\Omega) + D^2_{\mu,-2}(\Omega)\right)\right] + t_2\sqrt{\frac{2}{7}}\beta^2\left[-\cos 2\gamma D^2_{\mu 0}(\Omega) + \frac{\sin 2\gamma}{\sqrt{2}}\left(D^2_{\mu 2}(\Omega) + D^2_{\mu,-2}(\Omega)\right)\right]. \tag{2.49}$$

Table 11. The same as in table 6, but for ^{150}Nd. The experimental data are taken from [61].

^{150}Nd	Exp.	$X(5)$	ISW	D	SSA	CSM
2^+_g	130	124	121	124	111	130
4^+_g	381	361	358	384	348	386
6^+_g	720	675	682	738	683	734
8^+_g	1130	1054	1084	1158	1098	1149
10^+_g	1599	1494	1560	1625	1580	1618
12^+_g	2119	1993	2106	2129	2118	2133
14^+_g	2683	2549	2722	2664	2707	2688
0^+_β	675	702	580	739	630	675
2^+_β	851	926	783	863	822	852
4^+_β	1138	1328	1157	1123	1158	1167
6^+_β	1541	1833	1639	1477	1590	1541
8^+_β		2415	2209	1897	2095	1931
10^+_β		3067	2859	2364	2661	2319
2^+_γ	1062	1091	1087	1076	1091	1101
3^+_γ	1201	1198	1197	1195	1197	1191
4^+_γ	1353	1327	1333	1345	1328	1310
5^+_γ		1476	1491	1518	1474	1448
6^+_γ		1641	1671	1713	1663	1615
7^+_γ		1823	1872	1924	1838	1790
8^+_γ		2020	2093	2151	2079	1998
9^+_γ		2233	2334	2390	2276	2201
10^+_γ		2461	2594	2641	2561	2445
rms (keV)		114	48	28	29	20

The parameters t_1 and t_2 will be determined by the least-squares method. For the $X(5)$ model, in the limit of γ-small, only the harmonic part of the transition operator (2.49) is used:

$$T^{(E2)}_{2\mu,X(5)} = t\beta D^2_{\mu 0}(\Omega) + t\beta\frac{\gamma}{\sqrt{2}}(D^2_{\mu 2}(\Omega) + D^2_{\mu,2}(\Omega)). \tag{2.50}$$

The first term of equation (2.50) gives contributions only to $\triangle K = 0$ transitions, while the second term to $\triangle K = 2$ transitions. For $\triangle K = 0$ transitions, the matrix element of the γ variable is reduced to the orthogonality condition, while for $\triangle K = 2$ the γ matrix element can be considered as an intrinsic transition matrix element. Finally, the reduced transition probabilities will depend on two parameters [48]. Here, we will denote these two parameters with t and t' for $\triangle K = 0$ and $\triangle K = 2$ transitions, respectively.

3. The coherent state model

The CSM defines [5] first a restricted collective space whose vectors are model states of the ground, β and γ bands. In choosing these states, we were guided by some experimental information which results in formulating a set of criteria to be fulfilled by the searched states.

All these restrictions required are fulfilled by the following set of three deformed quadrupole boson states:

$$\psi_g = e^{[d(b^\dagger_0 - b_0)]}|0\rangle \equiv T|0\rangle, \quad \psi_\gamma = \Omega^\dagger_{\gamma,2}\psi_g, \quad \psi_\beta = \Omega^\dagger_\beta\psi_g, \tag{3.1}$$

Table 12. The same as in table 6, but for ^{156}Dy. The experimental data are taken from [63].

^{156}Dy	Exp.	$X(5)$	ISW	D	SSA	CSM
2_g^+	138	119	114	140	131	168
4_g^+	404	345	344	422	391	457
6_g^+	770	646	668	796	745	829
8_g^+	1216	1009	1079	1230	1175	1267
10_g^+	1725	1431	1572	1712	1667	1761
12_g^+	2286	1908	2145	2232	2151	2307
14_g^+	2888	2440	2796	2787	2807	2899
0_β^+	676	672	451	648	461	676
2_β^+	829	886	629	788	703	829
4_β^+	1088	1272	966	1070	1068	1102
6_β^+	1437	1755	1413	1444	1515	1452
8_β^+	1859	2313	1955	1878	2026	1859
10_β^+	2316	2937	2584	2360	2593	2312
2_γ^+	891	1069	898	839	928	921
3_γ^+	1022	1172	1004	970	1041	1024
4_γ^+	1168	1296	1136	1129	1188	1159
5_γ^+	1336	1438	1292	1312	1339	1312
6_γ^+	1525	1596	1472	1514	1542	1497
7_γ^+	1729	1771	1674	1732	1720	1686
8_γ^+	1959	1960	1899	1964	1972	1913
9_γ^+	2192	2163	2145	2210	2171	2131
10_γ^+	2448	2381	2413	2467	2464	2395
11_γ^+	2712	2613	2702	2735	2680	2636
12_γ^+	2997	2859	3013	3013	2949	2934
13_γ^+	3274	3118	3345	3301	3240	3153
14_γ^+		3391	3698	3600	3606	3526
15_γ^+	3861	3677	4071	3908	3847	3805
rms (keV)		232	114	35	90	41

where the excitation operators for β and γ bands are defined by

$$\Omega^\dagger_{\gamma,2} = (b^\dagger b^\dagger)_{2,2} + d\sqrt{\frac{2}{7}} b^\dagger_{2,2}, \quad \Omega^\dagger_\beta = (b^\dagger b^\dagger b^\dagger)_0 + \frac{3d}{\sqrt{14}}(b^\dagger b^\dagger)_0 - \frac{d^3}{\sqrt{70}}. \tag{3.2}$$

Here, d is a real parameter simulating the nuclear deformation. From the three deformed states, one generates through projection three sets of mutually orthogonal states

$$\varphi^i_{JM} = N^i_J P^J_{M0} \psi_i, \qquad i = g, \beta, \gamma, \tag{3.3}$$

where P^J_{MK} denotes the projection operator:

$$P^J_{MK} = \frac{2J+1}{8\pi^2} \int D^{J*}_{MK} \hat{R}(\Omega)\, \mathrm{d}\Omega, \tag{3.4}$$

N^i_J the normalization factors and D^J_{MK} the rotation matrix elements. The rotation operator corresponding to the Euler angles Ω is denoted by $\hat{R}(\Omega)$. It was proved that the deformed and projected states contain the salient features of the major collective bands. Since we attempt to set up a very simple model, we rely on the experimental feature saying that the β band is largely decoupled from the ground as well as from the γ bands and choose a model Hamiltonian whose

Table 13. The same as in table 6, but for ^{166}Hf. The experimental data are taken from [64].

^{166}Hf	Exp.	$X(5)$	ISW	D	SSA	CSM
2_g^+	159	164	164	152	149	177
4_g^+	470	476	476	471	458	488
6_g^+	897	891	890	906	883	897
8_g^+	1406	1391	1392	1415	1392	1385
10_g^+	1972	1973	1975	1973	1966	1943
12_g^+	2566	2631	2635	2566	2588	2568
0_β^+	1065	926	921	1064	1000	1098
2_β^+	1219	1222	1215	1216	1286	1219
4_β^+		1753	1745	1536	1761	1490
6_β^+		2419	2410	1970	2344	1870
8_β^+		3189	3178	2479	3002	2342
10_β^+		4049	4038	3038	3713	2893
2_γ^+	810	862	862	854	864	899
3_γ^+	1007	1004	1003	997	1007	1011
4_γ^+		1174	1174	1177	1178	1160
5_γ^+	1419	1370	1370	1385	1364	1330
6_γ^+		1589	1588	1617	1611	1535
7_γ^+		1829	1829	1867	1822	1748
8_γ^+		2090	2090	2133	2132	2002
9_γ^+		2370	2372	2411	2357	2251
10_γ^+		2671	2673	2701	2720	2550
rms (keV)		51	53	18	38	39

matrix elements between beta states and states belonging either to the ground or to the gamma band are all equal to zero. The simplest Hamiltonian obeying this restriction is

$$H = A_1(22\hat{N} + 5\Omega^\dagger_{\beta'}\Omega_{\beta'}) + A_2\hat{J}^2 + A_3\Omega^\dagger_\beta\Omega_\beta, \tag{3.5}$$

where $\hat{N}$ is the boson number, $\hat{J}^2$-angular momentum squared and $\Omega^\dagger_{\beta'}$ denotes

$$\Omega^\dagger_{\beta'} = (b^\dagger b^\dagger)_{00} - \frac{d^2}{\sqrt{5}}. \tag{3.6}$$

Higher order terms in boson operators can be added to the Hamiltonian H without altering the decoupling condition for the beta band. An example of this kind is the correction

$$\Delta H = A_4(\Omega^\dagger_\beta\Omega^2_{\beta'} + \text{h.c.}) + A_5\Omega^{\dagger 2}_{\beta'}\Omega^2_{\beta'}. \tag{3.7}$$

The energies for beta band and for the gamma band states of odd angular momentum are described as average values of H (3.5), or $H + \Delta H$ on φ^β_{JM} and φ^γ_{JM} (J-odd), respectively. As for the energies for the ground band and those of gamma band states with even angular momentum, they are obtained by diagonalizing a 2×2 matrix for each J.

The quadrupole transition operator is considered to be a sum of a linear term in bosons and one which is quadratic in the quadrupole bosons:

$$Q_{2\mu} = q_1(b^\dagger_{2\mu} + (-)^\mu b_{2,-\mu}) + q_2((b^\dagger b^\dagger)_{2\mu} + (bb)_{2\mu}) + q_3(b^\dagger b)_{2\mu}. \tag{3.8}$$

Note that if $q_3 = 2q_2$, the quadrupole transition operator can be obtained from the quadrupole transition operator expressed in terms of the collective quadruple coordinates $\alpha_{2\mu}$:

$$Q_{2\mu} = Q_1\alpha_{2\mu} + Q'_1(\alpha_2\alpha_2)_{2\mu}. \tag{3.9}$$

Table 14. The same as in table 6, but for ^{168}Hf. The experimental data are taken from [65].

^{168}Hf	Exp.	$X(5)$	ISW	D	SSA	CSM
2_g^+	124	141	140	120	108	128
4_g^+	386	409	409	382	351	389
6_g^+	757	765	769	757	710	756
8_g^+	1214	1195	1207	1215	1172	1206
10_g^+	1736	1694	1720	1736	1723	1730
12_g^+	2306	2259	2303	2307	2354	2320
0_β^+	942	795	755	928	878	942
2_β^+	1059	1049	1002	1048	1039	1049
4_β^+	1285	1505	1449	1310	1368	1285
6_β^+		2077	2015	1684	1823	1630
8_β^+		2738	2672	2143	2380	2068
10_β^+		3477	3412	2664	3024	2587
2_γ^+	876	911	906	902	928	939
3_γ^+	1031	1033	1028	1020	1042	1035
4_γ^+	1161	1179	1178	1172	1171	1161
5_γ^+	1386	1347	1350	1353	1334	1311
6_γ^+	1551	1535	1543	1558	1530	1492
7_γ^+		1741	1755	1786	1733	1687
8_γ^+		1965	1988	2033	1992	1916
9_γ^+		2206	2239	2297	2226	2148
10_γ^+		2464	2508	2576	2543	2421
rms (keV)		75	70	15	43	31

The anharmonic term in the above expression can be obtained by expanding the deformed mean field around the spherical equilibrium shape [50, 51] of the nuclear surface. For the near vibrational regime, the interband matrix elements of the q_3 term vanish within the CSM [5]. Moreover, a transition operator depending on two free parameters seems to be suitable for describing the $E2$ transition probabilities in several regions of the nuclide's chart [52].

Using the Rose convention [47], the reduced probability for the $E2$ transition $J_i^+ \to J_f^+$ can be expressed as

$$B(E2; J_i^+ \to J_f^+) = \left(\langle J_i^+ || Q_2 || J_f^+ \rangle\right)^2. \tag{3.10}$$

Three specific features of the CSM are worth mentioning.

(a) The model states are generated through projection from a coherent state and two excitations of that through simple polynomial boson operators. Thus, it is expected that the projected states may account for the semiclassical behavior of the nuclear system staying in a state of high spin.
(b) The states are an infinite series of bosons and thus highly deformed states can be described.
(c) The model Hamiltonian is not commuting with the boson number operator and because of this property a basis generated from a coherent state is expected to be most suitable.

The CSM has been successfully applied to several nuclei exhibiting various equilibrium shapes which, according to the IBA classification, exhibit the $SO(6)$, $SU(5)$ and $SU(3)$ symmetries. Several improvements of the CSM have been proposed by considering additional degrees of freedom such as isospin [6], quasi-particle [7] or collective octupole coordinates

Table 15. The same as in table 6, but for ^{170}W. The experimental data are taken from [66].

^{170}W	Exp.	$X(5)$	ISW	D	SSA	CSM
2^+_g	157	145	133	145	151	171
4^+_g	462	420	398	447	446	475
6^+_g	876	785	767	858	844	873
8^+_g	1363	1226	1228	1347	1323	1346
10^+_g	1902	1739	1777	1894	1869	1882
12^+_g	2464	2319	2411	2489	2471	2477
14^+_g	3118	2965	3128	3126	3124	3128
16^+_g	3816	3677	3927	3801	3821	3831
0^+_β		816	587	760	507	823
2^+_β	953	1077	804	905	790	953
4^+_β	1202	1545	1208	1207	1204	1215
6^+_β	1578	2132	1736	1618	1706	1578
8^+_β		2810	2367	2107	2277	2020
10^+_β		3568	3093	2654	2905	2531
2^+_γ	937	944	945	928	936	965
3^+_γ	1074	1068	1068	1066	1064	1074
4^+_γ	1220	1219	1219	1238	1231	1217
5^+_γ		1391	1397	1438	1400	1381
6^+_γ		1584	1600	1662	1630	1578
7^+_γ		1796	1828	1906	1828	1783
8^+_γ		2025	2080	2168	2109	2027
9^+_γ		2273	2355	2446	2329	2264
10^+_γ		2538	2653	2739	2655	2550
rms (keV)		200	90	21	58	13

[8, 9]. The CSM has also been used to describe some nonaxial nuclei [49], and the results were compared with those obtained with the rotationvibration model [2]. A review of the CSM achievements is found in [10]. The terms involved in the model Hamiltonians used in by the CSM [5] and its generalized version [6] have microscopic counterparts as shown in [11] and [12], respectively.

4. Numerical results

4.1. Parameters

The parameters which define the energies and the $E2$ transition probabilities of the models $X(5)$, ISW, D, SSA and CSM were fitted by the least-squares method for ten nuclei: ^{176,178,180,188,190}Os, ^{150}Nd, ^{156}Dy, ^{166,168}Hf and ^{170}W. In the least-squares procedure, all experimental energies were considered. The resulting values are those given in tables 1–5. For the first three and the last three nuclei from table 1, the parameter t' cannot be determined since the corresponding term from the transition operator does not contribute to the intraband decays.

Some parameters vary by a large amount from one isotope to another but the relative variation is small. For example in the case of Os isotopes, the parameters could be interpolated

Table 16. The reduced $E2$ transition probabilities determined with the $X(5)$, ISW, D, SSA and CSM models for the ^{176}Os nucleus are compared with the corresponding experimental data taken from [54].

B(E2)(W.u.)	Exp.	$X(5)$	ISW	D	SSA	CSM
$2_g^+ \to 0_g^+$	144^{+5}_{-5}	167	127	145	136	144
$4_g^+ \to 2_g^+$	243^{+5}_{-5}	264	224	228	227	253
$6_g^+ \to 4_g^+$	305^{+11}_{-11}	330	305	292	297	328
$8_g^+ \to 6_g^+$	321^{+15}_{-14}	379	377	360	366	393
$10_g^+ \to 8_g^+$	441^{+88}_{-63}	419	438	433	435	452
$12_g^+ \to 10_g^+$	517^{+336}_{-146}	450	490	510	504	517

Table 17. The same as in table 16, but for ^{178}Os. The experimental data are taken from [54–56]

B(E2)(W.u.)	Exp.	$X(5)$	ISW	D	SSA	CSM
$2_g^+ \to 0_g^+$	138	147	137	146	141	138
$4_g^+ \to 2_g^+$	226	232	225	226	226	227
$6_g^+ \to 4_g^+$	290	291	287	280	283	282
$8_g^+ \to 6_g^+$	327	334	337	332	334	327
$10_g^+ \to 8_g^+$	384	369	378	384	382	368

Table 18. The same as in table 16, but for ^{180}Os. The experimental data are taken from [58].

B(E2)(W.u.)	Exp.	$X(5)$	ISW	D	SSA	CSM
$2_g^+ \to 0_g^+$	120^{+30}_{-30}	70	152	148	151	150
$4_g^+ \to 2_g^+$	193^{+25}_{-25}	111	167	177	172	149
$6_g^+ \to 4_g^+$	160^{+40}_{-40}	139	132	139	135	120
$8_g^+ \to 6_g^+$	63^{+13}_{-13}	160	95	83	90	96

by smooth curves. One parameter falls aside namely those of ^{188}Os, which seems to achieve the critical point of the shape transition, i.e. exhibits an $X(5)$ behavior.

We note that the parameter F involves the average value $\langle\beta^2\rangle$ which, in principle, is an angular-momentum-dependent quantity. Therefore, the differential equation in γ should be iteratively solved, at each step the inserted average value being calculated with the wavefunction provided in the previous step. When the convergence of the process is met, one keeps the average value for the chosen angular momentum. Here, $\langle\beta^2\rangle$ was kept constant. Whether this hypothesis is valid or not can be posterity checked. To this goal, we represented in figure 1, the average $\langle\beta^2\rangle$ for each of the models ISW, D and SSA. We note that the average value only slightly depends on J and that is especially true for ISW and SSA. If the limit of $\langle\beta^2\rangle$, when the convergence of the iterations mentioned above is reached, depends on J like the averages shown in figure 1, one could say that keeping $\langle\beta^2\rangle$ constant one ignores a slight decrease of energy with angular momentum.

With the parameters listed above the potentials in the variables β and γ and the wavefunctions describing the low lying states from the ground, beta and gamma bands respectively, are represented for four nuclei, as shown in figures 2–5. Analyzing these figures, several features can be noted. The β potential has a deformed minimum located at a deformation which differs from one nucleus to another. The wavefunctions in β for 0_g^+ and 2_γ^+ are almost

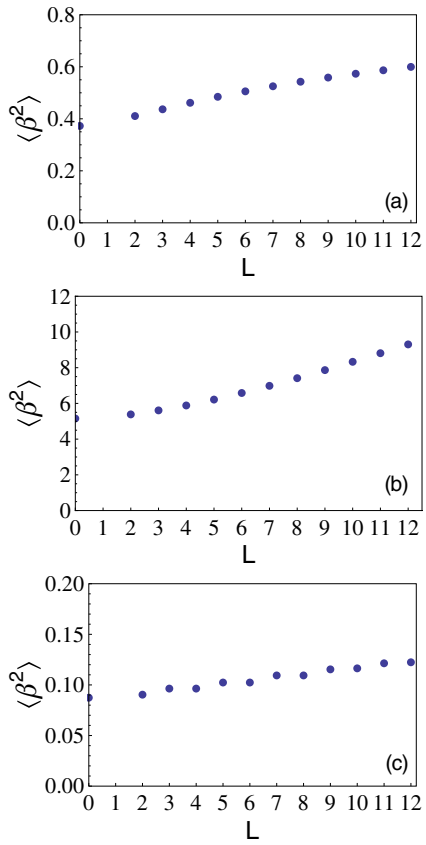

Figure 1. The average values of β^2 versus the angular momentum calculated within the ISW (panel a)), the D (panel b)) and the SSA (panel c)) models.

identical and have only one maximum and no node, while the band for 0^+_β has one node, one maximum and one minimum. The maximum of the $|\phi|^2$ distribution for the three states represented in the quoted figures is achieved at a point which is close to the potential minimum. If $|\phi|^2$ is multiplied with the integration measure over β, then the probability distribution has a maximum closer to the potential minimum. The state 0^+_β is characterized by two maxima for the probability distribution of the beta variable. This feature reflects the specific structure of the excitation operator of this state, from the ground state, i.e. $n_\beta = 1$. The behavior of the wavefunctions in the variable γ is mainly determined by the discontinuity for $\gamma = 0$ and $\gamma = \frac{\pi}{3}$. The potential has two minima, one well pronounced near the first wall and one very flat close to the $\gamma = \frac{\pi}{3}$ discontinuity. Due to this structure, the wavefunction describing a state in the ground band has two maxima located above the mentioned minima. The state 2^+_γ heading the gamma band has an additional maximum.

4.2. Energies

The spectra of the chosen nuclei, determined by the models $X(5)$, ISW, D, SSA and CSM, are compared with the corresponding experimental data in tables 6–15. The quality of agreement between the results of our calculations and the corresponding experimental data is given by

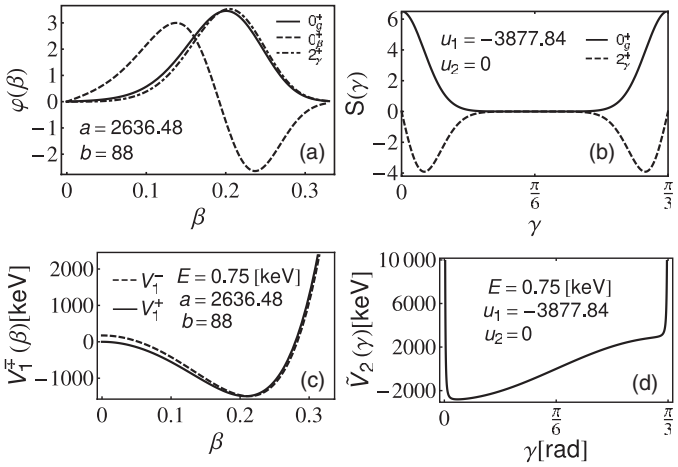

Figure 2. The solutions for the equation in β, corresponding to various angular momenta and the potential from the left-bottom panel, are plotted, in panel left-up, as a function of β. Similarly, on the right column the wavefunctions for γ for different angular momenta and the effective potential shown in the right-bottom panel are plotted as a function of γ. The results correspond to ^{150}Nd.

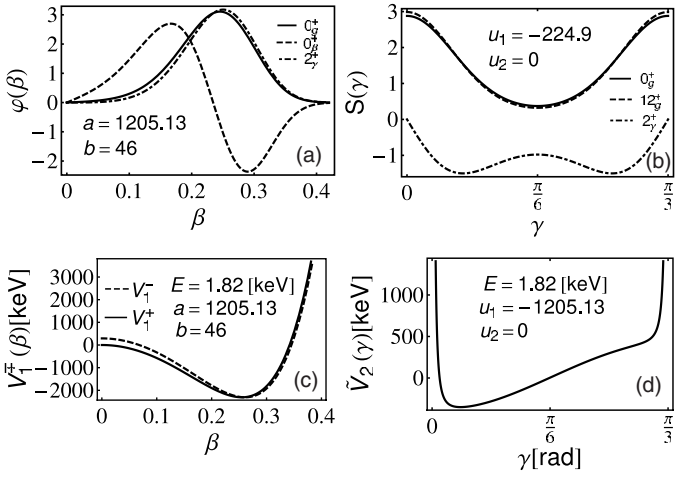

Figure 3. The same as in figure 2, but for ^{166}Hf.

the rms values of the deviations. Thus, comparing the rms values corresponding to different models we conclude that for ^{180}Os, ^{150}Nd and ^{170}W the best description of the spectra is that given by the CSM approach, energies of ^{188}Os calculated with the SSA are closest to the experimental ones, while for the remaining nuclei the D formalism provides the most realist picture.

Using the experimental data listed in tables 6–15, one can calculate the ratio of the excitation energies for the states 4_g^+ and 2_g^+, denoted by $R_{4_g^+/2_g^+}$. The results are 2.93 (^{176}Os, ^{190}Os, ^{150}Nd, ^{156}Dy), 2.94 (^{170}W), 2.96 (^{166}Hf), 3.02 (^{178}Os), 3.08 (^{188}Os), 3.10 (^{180}Os) and 3.11 (^{168}Hf). We note that all nuclei are characterized by a ratio $R_{4_g^+/2_g^+}$ which is close to the

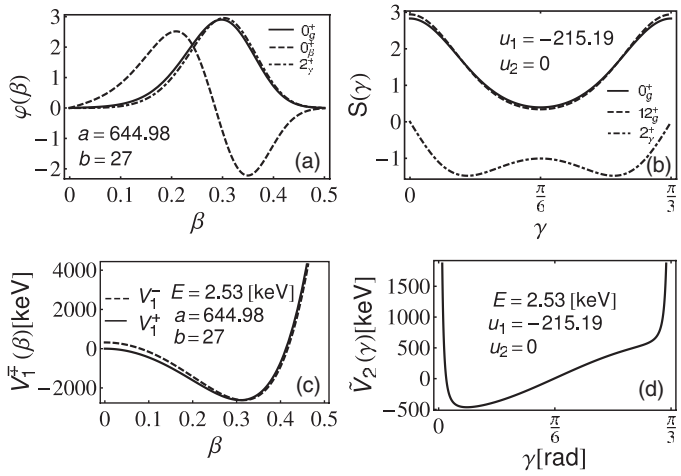

Figure 4. The same as in figure 2, but for ^{188}Os.

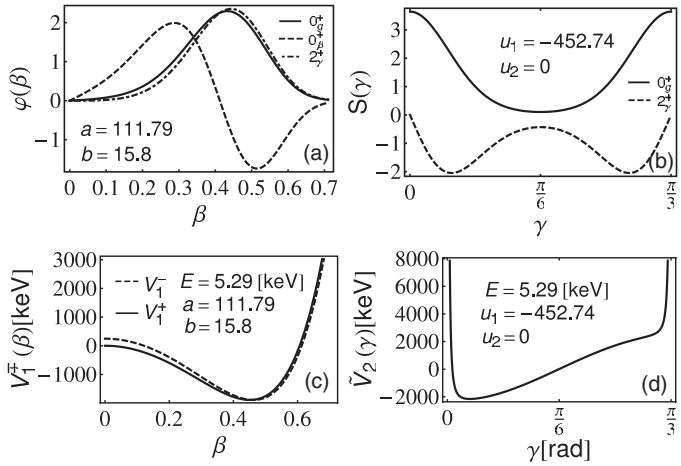

Figure 5. The same as in figure 2, but for ^{190}Os.

value of 2.9 assigned to the critical point of the transition $SU(5)\rightarrow SU(3)$, which is described by the solvable model called $X(5)$. Despite this, the $X(5)$ approach provides a description which is worse than those obtained with the other models proposed here.

4.3. Reduced transition probabilities

As mentioned before, the parameters involved in the transition operators employed by different models have been fixed by fitting through a least-squares procedure the existent data. With the fitted parameter, the results for the reduced $E2$ transition probabilities are presented in tables 16–25 where one also gives for comparison the available experimental data. For the lightest three isotopes of Os as well as for ^{166,168}Hf and ^{170}W, the available experimental data

Table 19. The same as in table 16, but for ^{188}Os. The experimental data are taken from [59].

B(E2)(W.u.)	Exp.	$X(5)$	ISW	D	SSA	CSM
$2_g^+ \to 0_g^+$	79^{+2}_{-2}	74	72	79	82	42
$4_g^+ \to 2_g^+$	133^{+8}_{-8}	118	115	121	123	87
$6_g^+ \to 4_g^+$	138^{+8}_{-8}	147	144	147	145	125
$8_g^+ \to 6_g^+$	161^{+11}_{-11}	169	166	174	162	161
$10_g^+ \to 8_g^+$	188^{+25}_{-25}	187	184	203	178	195
$0_\beta^+ \to 2_g^+$	$0.95^{+0.08}_{-0.08}$	47	48	33	21	0.95
$0_\beta^+ \to 2_\gamma^+$	$4.3^{+0.5}_{-0.5}$	5.2	5.2	1.9	1.5	44
$4_\gamma^+ \to 2_\gamma^+$	47^{+10}_{-10}	47	50	52	56	14
$4_\gamma^+ \to 3_\gamma^+$	320^{+120}_{-120}	112	117	120	132	43
$6_\gamma^+ \to 4_\gamma^+$	70^{+30}_{-30}	107	111	114	118	31
$2_\gamma^+ \to 0_g^+$	$5^{+0.6}_{-0.6}$	8.4	10.9	10.8	9.9	5
$2_\gamma^+ \to 2_g^+$	16^{+2}_{-2}	13	17	16	14	10.4
$2_\gamma^+ \to 4_g^+$	34^{+5}_{-5}	0.65	0.85	0.80	0.73	1.4
$4_\gamma^+ \to 2_g^+$	$1.29^{+0.19}_{-0.19}$	5.7	7.1	6.7	6.1	1.7
$4_\gamma^+ \to 4_g^+$	19^{+3}_{-3}	18	23	20	19	10.7
$4_\gamma^+ \to 6_g^+$	16^{+7}_{-7}	2	2	2	2	5
$6_\gamma^+ \to 4_g^+$	$0.21^{+0.11}_{-0.11}$	5.3	6.4	5.8	5.3	0.9
$6_\gamma^+ \to 6_g^+$	>9.4	21	25	23	20	8.3

Table 20. The same as in table 16, but for ^{190}Os. The experimental data are taken from [60].

B(E2)(W.u.)	Exp.	$X(5)$	ISW	D	SSA	CSM
$2_g^+ \to 0_g^+$	72^{+2}_{-2}	58	57	56	61	45
$4_g^+ \to 2_g^+$	105^{+6}_{-6}	91	91	88	94	83
$6_g^+ \to 4_g^+$	113^{+10}_{-10}	115	113	112	112	112
$8_g^+ \to 6_g^+$	137^{+20}_{-20}	131	130	138	126	137
$10_g^+ \to 8_g^+$	120^{+30}_{-30}	145	143	165	139	160
$0_\beta^+ \to 2_g^+$	$2.2^{+0.5}_{-0.5}$	36	36	30	19	2.2
$0_\beta^+ \to 2_\gamma^+$	23^{+7}_{-7}	8.9	9	8	5	148
$4_\gamma^+ \to 2_\gamma^+$	53^{+5}_{-5}	36	38	37	41	20.4
$4_\gamma^+ \to 3_\gamma^+$	65^{+13}_{-13}	87	90	87	98	84
$6_\gamma^+ \to 4_\gamma^+$	65^{+13}_{-13}	83	85	84	89	49
$8_\gamma^+ \to 6_\gamma^+$	61^{+16}_{-16}	112	113	119	115	72
$2_\gamma^+ \to 0_g^+$	$5.9^{+0.6}_{-0.6}$	14.2	15.6	15.9	16.2	14
$2_\gamma^+ \to 2_g^+$	33^{+4}_{-4}	21	24	24	24	33
$4_\gamma^+ \to 2_g^+$	$0.68^{+0.06}_{-0.06}$	9.7	10.3	10.4	10.3	4.3
$4_\gamma^+ \to 4_g^+$	30^{+4}_{-4}	31	33	33	32	31
$6_\gamma^+ \to 4_g^+$	<0.8	9	10	10	9	1.7
$6_\gamma^+ \to 6_g^+$	31^{+8}_{-8}	36	38	40	36	26

refer to the states of ground band. Agreements with the experimental data showed up by the five theoretical models are comparable in quality.

For ^{156}Dy, besides the intraband transitions in the ground band, a few interband transitions from the gamma to the ground band are experimentally known. As seen from table 22, agreement between calculations with the experimental data is quite good.

Table 21. The same as in table 16, but for ^{150}Nd. The experimental data are taken from [62].

B(E2)(W.u.)	Exp.	$X(5)$	ISW	D	SSA	CSM
$2_g^+ \to 0_g^+$	115^{+2}_{-2}	107	104	92	116	81
$4_g^+ \to 2_g^+$	182^{+2}_{-2}	169	168	144	177	160
$6_g^+ \to 4_g^+$	210^{+2}_{-2}	212	210	183	211	222
$8_g^+ \to 6_g^+$	278^{+25}_{-25}	243	243	224	240	278
$10_g^+ \to 8_g^+$	204^{+12}_{-12}	269	269	268	266	330
$2_\beta^+ \to 0_\beta^+$	114^{+23}_{-23}	85	83	130	86	116
$4_\beta^+ \to 2_\beta^+$	170^{+51}_{-51}	128	125	194	144	165
$0_\beta^+ \to 2_g^+$	39^{+2}_{-2}	67	73	51	37	41.2
$2_\beta^+ \to 0_g^+$	$1.2^{+0.2}_{-0.2}$	2.1	2.9	3.1	1.6	5.2
$2_\beta^+ \to 2_g^+$	9^{+2}_{-2}	10	10	9	6	9
$2_\beta^+ \to 4_g^+$	17^{+3}_{-3}	39	42	40	26	26
$4_\beta^+ \to 2_g^+$	$0.12^{+0.02}_{-0.02}$	1.07	1.61	1.64	0.57	5.6
$4_\beta^+ \to 4_g^+$	7^{+1}_{-1}	6	8	8	5	7.2
$4_\beta^+ \to 6_g^+$	70^{+13}_{-13}	30	33	46	26	26
$2_\gamma^+ \to 0_g^+$	$3^{+0.8}_{-0.8}$	2.4	8	9.8	5.1	16.3
$2_\gamma^+ \to 2_g^+$	$5.4^{+1.7}_{-1.7}$	3.6	11.9	14.3	7.3	5.4
$2_\gamma^+ \to 4_g^+$	$2.6^{+2.0}_{-2.0}$	0.2	0.6	0.7	0.4	0.74
$4_\gamma^+ \to 2_g^+$	$0.9^{+0.3}_{-0.3}$	1.6	5	6.1	3	28.6
$4_\gamma^+ \to 4_g^+$	$3.9^{+1.2}_{-1.2}$	5.3	15.5	18.9	9	9.6

Table 22. The same as in table 16, but for ^{156}Dy. The experimental data are taken from [63].

B(E2)(W.u.)	Exp.	$X(5)$	ISW	D	SSA	CSM
$2_g^+ \to 0_g^+$	$149.3^{+2.5}_{-2.5}$	142	138	111	137	66
$4_g^+ \to 2_g^+$	261^{+17}_{-17}	225	223	179	219	149
$6_g^+ \to 4_g^+$	200^{+15}_{-15}	282	279	235	271	221
$8_g^+ \to 6_g^+$	289^{+14}_{-14}	323	323	295	316	289
$10_g^+ \to 8_g^+$	366^{+25}_{-25}	358	358	359	357	354
$12_g^+ \to 10_g^+$	382^{+22}_{-22}	385	386	425	395	418
$2_\gamma^+ \to 0_g^+$	$7.2^{+0.4}_{-0.4}$	6.6	9.9	23.3	11.6	7.2
$2_\gamma^+ \to 2_g^+$	$9.4^{+1.0}_{-1.0}$	9.8	14.6	35.1	17.4	9.4
$2_\gamma^+ \to 4_g^+$	$12.6^{+1.9}_{-1.9}$	0.5	0.7	1.8	0.9	19.5

In [62], measured data in ^{150}Nd for intraband transitions ground to ground and beta to beta as well interband transitions to ground band have been reported. These data are described reasonably well by the five approaches as shown in table 21. One remarks the good agreement obtained with the CSM approach. The largest discrepancies with the experimental data are obtained for the transitions $4_\beta^+ \to 2_g^+$ and $4_\gamma^+ \to 2_g^+$ which are overestimated by the theoretical results.

As for ^{188,190}Os, the available data are about the intraband transitions ground to ground and gamma to gamma bands as well about the interband transition beta to ground and gamma to ground. They are compared with the results of our calculations in tables 19 and 20. Again, the agreement qualities obtained with the five sets of calculations are comparable with each other. The predictions for the decay probabilities of the transitions $4_\gamma^+ \to 2_g^+$ and $6_\gamma^+ \to 4_g^+$

Table 23. The same as in table 16, but for ^{166}Hf. The experimental data are taken from [64].

B(E2)(W.u.)	Exp.	$X(5)$	ISW	D	SSA	CSM
$2_g^+ \to 0_g^+$	128^{+7}_{-7}	98	153	154	155	128
$4_g^+ \to 2_g^+$	202^{+7}_{-7}	155	212	216	215	203
$6_g^+ \to 4_g^+$	221^{+13}_{-13}	194	225	232	226	245
$8_g^+ \to 6_g^+$	280^{+30}_{-30}	223	225	230	225	280
$10_g^+ \to 8_g^+$	250^{+640}_{-110}	246	220	219	218	311
$12_g^+ \to 10_g^+$	155^{+550}_{-70}	265	213	199	209	351

Table 24. The same as in table 16, but for ^{168}Hf. The experimental data are taken from [65].

B(E2)(W.u.)	Exp.	$X(5)$	ISW	D	SSA	CSM
$2_g^+ \to 0_g^+$	154^{+7}_{-7}	141	165	176	175	154
$4_g^+ \to 2_g^+$	244^{+12}_{-12}	223	250	257	255	249
$6_g^+ \to 4_g^+$	285^{+18}_{-18}	279	294	292	291	304
$8_g^+ \to 6_g^+$	350^{+50}_{-50}	320	322	318	316	350
$10_g^+ \to 8_g^+$	370^{+60}_{-60}	354	342	338	338	391
$12_g^+ \to 10_g^+$	320^{+120}_{-120}	381	356	354	357	438

Table 25. The same as in table 16, but for ^{170}W. The experimental data are taken from [66].

B(E2)(W.u.)	Exp.	$X(5)$	ISW	D	SSA	CSM
$2_g^+ \to 0_g^+$	124^{+3}_{-3}	79	133	126	129	124
$4_g^+ \to 2_g^+$	179^{+18}_{-18}	125	179	177	179	168
$6_g^+ \to 4_g^+$	189^{+14}_{-14}	157	184	189	187	182
$8_g^+ \to 6_g^+$	190^{+50}_{-50}	180	180	187	183	190
$10_g^+ \to 8_g^+$	170^{+40}_{-40}	199	173	175	174	197
$12_g^+ \to 10_g^+$	160^{+30}_{-30}	214	167	158	162	214

are larger than the corresponding experimental data. Also, the result for $0_\beta^+ \to 2_\gamma^+$ obtained within the CSM is about 6.5 larger than the corresponding experimental value. For some cases, the value of the t_2 obtained through the least-squares procedure is very large. The reason is as follows.

Within the SSA, the t_2 term of the transition operator contributes mainly to the interband transitions, while its matrix elements between states of a given band are very small. However, for the mentioned cases there are only few experimental data for interband transitions, most of the data referring to the intraband transitions. Consequently, the least-squares procedure uses small matrix elements of the intraband transitions which results in obtaining a huge number for t_2. An equally good description of these cases would be obtained by ignoring the t_2 term. We kept however this term just for the sake of having an unitary approach.

The results for the $E2$ transitions raise the question: Why the models $X(5)$, ISW, D, SSA predict close results, although the states involved are described by different wavefunctions in the variables β and γ? It seems that these differences are washed out by the fitting procedure adopted for the strengths of the transition operator. Moreover, the factor function depending

on the Euler angles are common in the mentioned four approaches, thus giving the dominant contribution to the reduced transition probability.

One signature for the triaxiality of the nuclear shape is the equality:

$$E_{2_1^+} + E_{2_2^+} = E_{3_1^+}. \tag{4.1}$$

The departure from this rule, $\Delta E = |E_{2_1^+} + E_{2_2^+} - E_{3_1^+}|$, is equal to 2 and 11 keV for ^{188}Os and ^{190}Os, respectively. The magnitude of these deviations was the argument for treating the two isotopes as triaxial nuclei [44]. On the other hand, the ratio $E_{4/2}$ amounts to 2.93 and 3.08 for ^{188}Os and ^{190}Os, respectively, which are quite close to the specific value of $X(5)$ nuclei. Given these facts, we asked ourselves whether these nuclei are axially symmetric or behave like a triaxial rigid rotor. In order to answer this question, we compared the rms values of deviations for both energies and $B(E2)$ values provided by the SMA and SSA approaches, respectively. Concerning the excitation energies in the three major bands, the rms values of prediction deviations from the corresponding experimental data yielded by the SMA for ^{188}Os and ^{190}Os are 24 and 32 keV, respectively, while the SSA results for these values being 13 and 27 keV, respectively. Therefore, regarding the excitation energies the two isotopes behave more like axially deformed nuclei. However, comparing the results for the reduced transition probabilities, it comes out that the triaxial rigid rotor behavior is favored. Indeed, the rms values for the SMA approach applied to ^{188}Os and ^{190}Os are 13 and 16 W.u., respectively, while those corresponding to the SSA are 16 and 17 W.u., respectively. Remarkable is the fact that the differences of the rms values characterizing the two approaches, SMA and SSA, are quite small. Therefore, one could conclude that the two investigations, from [44] and from here, indicate that the two nuclei might be equally well described by both approaches.

5. Conclusions

Here, we summarize the main results obtained by this work. We selected ten nuclei characterized by a ratio $R_{4_g^+/2_g^+}$ close to 2.9 which is specific to the so-called $X(5)$ nuclei. Spectra of these nuclei are described by a new approach which treats the beta variable by the Schrödinger equation associated with a sextic oscillator plus a centrifugal potential. For the variable γ, one finds a differential equation which is satisfied by the spheroidal function. The excitation energies are obtained by summing the eigenvalues provided by the differential equations for the β and γ variables, respectively, while the corresponding functions are used to calculate the $E2$ transition probabilities. The results are compared with the corresponding experimental data as well as with those obtained through other formalisms called $X(5)$, ISW, D and CSM which were previously used by the present authors to describe the spectroscopic properties of other $X(5)$ like nuclei.

Note that while the formalisms $X(5)$, ISW, D and SSA treat the energies and transition probabilities using the intrinsic coordinates and the rotation matrix function, the CSM is a quadrupole boson approach and therefore the mentioned observables are calculated with the collective coordinates which are specific to the laboratory frame.

A comparison of the rms values yielded by the five approaches shows that the D, CSM and SSA approaches produce the best agreement with the experimental energies. Concerning the $E2$ transitions, one may show that all five sets of results quantitatively describe the experimental situation in a comparable manner with a slight advantage for SSA and CSM. Since the formalisms ISW, D, and SSA differ from each other by the way the variable beta is treated, otherwise the γ equation being the same, the transition probabilities produced by the three approaches exhibit similar agreement with the experimental data. The SSA method produces very good agreement with the experimental energies for ^{188}Os, ^{150}Nd and ^{168}Hf.

Table 5 shows that these nuclei have the largest deformations and moreover for the first two nuclei the ratio $R_{4^+/2^+}$ has the values 3.08 and 3.11, respectively, which deviate most from the $X(5)$ value. The quoted ratio for ^{150}Nd is 2.93, which is close to the $X(5)$ value but its deformation is the largest one.

The sextic potential for the β ensures a more realistic description of the excited states where the excitation of the beta degree of freedom is important. This is best seen in the excellent agreement of the calculated excitation energies in the beta and gamma bands with the corresponding experimental data.

The final conclusion is that the SSA, proposed in this paper, proves to be a suitable tool for a realistic description of the $X(5)$ like nuclei.

Acknowledgments

This work was supported by the Romanian Ministry for Education Research Youth and Sport through the CNCSIS project ID-2/5.10.2011.

References

[1] Bohr A 1952 *Mat.-Fys. Medd. K. Dan. Vidensk. Selsk.* **16** 1
Bohr A and Mottelson B 1953 *Mat.-Fys. Medd. K. Dan. Vidensk. Selsk.* **27** 1
[2] Faessler A and Greiner W 1962 *Z. Phys.* **168** 425
Faessler A and Greiner W 1962 *Z. Phys.* **170** 105
Faessler A and Greiner W 1964 *Z. Phys.* **177** 190
Faessler A, Greiner W and Sheline R 1965 *Nucl. Phys.* **70** 33
[3] Gneuss G, Mosel U and Greiner W 1969 *Phys. Lett.* B **30** 397
[4] Hess P, Maruhn J and Greiner W 1981 *Phys. Rev.* C **23** 2335
Hess P, Maruhn J and Greiner W 1981 *J. Phys. G: Nucl. Phys.* **7** 737
[5] Raduta A A, Ceausescu V, Gheorghe A and Dreizler R M 1981 *Phys. Lett.* B **99** 444
Raduta A A, Ceausescu V, Gheorghe A and Dreizler R M 1982 *Nucl. Phys.* A **381** 253
[6] Raduta A A, Ceausescu V and Faessler A 1987 *Phys. Rev.* C **36** 2111
[7] Raduta A A, Lima C and Faessler A 1983 *Z. Phys.* A **313** 69
[8] Raduta A A, Raduta Al H and Faessler A 1997 *Phys. Rev.* C **55** 1747
Raduta A A, Ionescu D and Faessler A 2002 *Phys. Rev.* C **65** 064322
[9] Raduta A A and Sabac C 1983 *Ann. Phys., NY* **148** 1
[10] Raduta A A 2004 *Recent Research Developments in Nuclear Physics* vol 1 pp 1–70 ISBN:81-7895-124-X (managing editor: S G Pandalai, Transworld Research Network)
[11] Ceausescu V and Raduta A A 1976 *Ann. Phys., NY* **100** 94
[12] Raduta A A, Simkovic F and Faessler A 2000 *J. Phys. G: Nucl. Part. Phys.* **26** 793
[13] Wilets L and Jean M 1956 *Phys. Rev.* **102** 788
[14] Davydov A S and Filippov G F 1958 *Nucl. Phys.* **8** 237
[15] Arima A and Iachello F 1976 *Ann. Phys., NY* **99** 253
Arima A and Iachello F 1979 *Ann. Phys., NY* **123** 468
[16] Iachello F and Arima A 1987 *The Interacting Boson Model* (Cambridge: Cambridge University Press)
[17] Ginocchio J H and Kirson M W 1980 *Phys. Rev. Lett.* **44** 1744
[18] Dieperink A E L, Scholten O and Iachello F 1980 *Phys. Rev. Lett.* **44** 1767
[19] McCutchan E A, Zamfir N V and Casten R F 2004 *Phys. Rev.* C **69** 064306
[20] McCutchan E A and Zamfir N V 2005 *Phys. Rev.* C **71** 054306
[21] Iachello F 2000 *Phys. Rev. Lett.* **85** 3580
[22] Iachello F 2001 *Phys. Rev. Lett.* **87** 052502
[23] Casten R F and Zamfir N V 2000 *Phys. Rev. Lett.* **85** 3584
[24] Casten R F and Zamfir N V 2001 *Phys. Rev. Lett.* **87** 052503
[25] Zamfir N V *et al* 2002 *Phys. Rev.* C **65** 044325
[26] Clark R M *et al* 2004 *Phys. Rev.* C **69** 064322
[27] Zhang D-l and Liu Y-x 2002 *Phys. Rev.* C **65** 057301
[28] Bonatsos D, Lenis D, Minkov N, Petrellis D, Raychev P P and Terziev P A 2003 arXiv:nucl-th/0312121v1
Bonatsos D, Lenis D, Minkov N, Petrellis D, Raychev P P and Terziev P A 2004 *Phys. Lett.* B **584** 40

[29] Davidson P M 1932 *Proc. R. Soc.* **135** 459
[30] Raduta A A, Gheorghe A and Faessler A 2005 *J. Phys. G: Nucl. Part. Phys.* **31** 337
[31] Leyvraz F and Heiss W D 2005 *Phys. Rev. Lett.* **95** 050402
[32] Gilmore R and Feng D H 1978 *Nucl. Phys.* A **301** 189
[33] Caprio M A, Cejnar P and Iachello F 2008 *Ann. Phys., NY* **323** 1106
[34] Fortunato L 2005 *Eur. J. Phys.* A **26** 1–30
[35] Gheorghe A, Raduta A A and Ceausescu V 1978 *Nucl. Phys.* A **296** 228
[36] Raduta A A, Gheorghe A and Ceausescu V 1978 *Nucl. Phys.* A **311** 118
[37] Chacon E, Moshinski M and Sharp R T 1976 *J. Math. Phys.* **17** 668
[38] Corrigan T M, Margetan F J and Williams S A 1976 *Phys. Rev.* C **14** 2279
[39] Margetan T M and Williams S A 1982 *Phys. Rev.* C **25** 1602
[40] Gheorghe A, Raduta A A and Ceausescu V 1998 *Nucl. Phys.* A **637** 201
[41] Gheorghe A, Raduta A A and Faessler A 2007 *Phys. Lett.* B **648** 171
[42] Raduta A A, Gheorghe A C, Buganu P and Faessler A 2009 *Nucl. Phys.* A **819** 46
[43] Cejnar P, Jolie J and Casten R F 2010 *Rev. Mod. Phys.* **82** 2155
[44] Raduta A A and Buganu P 2011 *Phys. Rev.* C **83** 034313
[45] Ushveridze A G 1994 *Quasi-Exactly Solvable Models in Quantum Mechanics* (Bristol: IOP)
[46] Lévai G and Arias J M 2004 *Phys. Rev.* C **69** 014304
[47] Rose M E 1957 *Elementary Theory of Angular Momentum* (New York: Wiley)
[48] Bijker R, Casten R F, Zamfir N V and McCutchan E A 2003 *Phys. Rev.* C **68** 064304
[49] Meyer U, Raduta A A and Faessler A 1998 *Nucl. Phys.* A **637** 321
[50] Raduta A A, Ceausescu V and Dreizler R M 1976 *Nucl. Phys.* A **272** 11
[51] Greiner W and Maruhn J *Nuclear Models* (Berlin: Springer) p 132 ISBN 3-540-59180-X
[52] Raduta A A, Budaca R and Faessler A 2012 *Ann. Phys., NY* **327** 671–704
[53] Basunia M S 2006 *Nucl. Data Sheets* **107** 791
[54] Melon B 2011 *Investigation of the X(5)-structure in* ^{176}*Os using absolute transition probabilities Inaugural-Dissertation zur Erlangung des Doktorgrades der Mathematisch-Naturwissenschaftlochen* Facultät der Universität zu Köln
[55] Kibédi T, Dracoulis G D, Byrne A P and Davidson P M 1994 *Nucl. Phys.* A **567** 183
[56] Möller O *et al* 2005 *Phys. Rev.* C **72** 034306
[57] Achterberg E, Capurro O A and Marti G V 2009 *Nucl. Data Sheets* **110** 1473
[58] Wu S-C and Niu H 2003 *Nucl. Data Sheets* **100** 483
[59] Singh B 2002 *Nucl. Data Sheets* **95** 387
[60] Singh B 2003 *Nucl. Data Sheets* **99** 275
[61] Dermateosian E and Tuli J K 1995 *Nucl. Data Sheets* **75** 827
[62] Krücken R *et al* 2002 *Phys. Rev. Lett.* **88** 232501
[63] Reich C W 2003 *Nucl. Data Sheets* **99** 753
[64] Baglin C M 2008 *Nucl. Data Sheets* **109** 1103
[65] Baglin C M 2010 *Nucl. Data Sheets* **111** 1807
[66] Baglin C M 2002 *Nucl. Data Sheets* **96** 611